Cellular/Molecular

Ca^{2+} Diffusion through Endoplasmic Reticulum Supports Elevated Intraterminal Ca^{2+} Levels Needed to Sustain Synaptic Release from Rods in Darkness

Minghui Chen,[1,2] Matthew J. Van Hook,[2] and Wallace B. Thoreson[1,2]

Departments of [1]Pharmacology and Experimental Neuroscience and [2]Ophthalmology and Visual Sciences, Truhlsen Eye Institute, University of Nebraska Medical Center, Omaha, Nebraska 68198

In addition to vesicle release at synaptic ribbons, rod photoreceptors are capable of substantial slow release at non-ribbon release sites triggered by Ca^{2+}-induced Ca^{2+} release (CICR) from intracellular stores. To maintain CICR as rods remain depolarized in darkness, we hypothesized that Ca^{2+} released into the cytoplasm from terminal endoplasmic reticulum (ER) can be replenished continuously by ions diffusing within the ER from the soma. We measured $[Ca^{2+}]$ changes in cytoplasm and ER of rods from *Ambystoma tigrinum* retina using various dyes. ER $[Ca^{2+}]$ changes were measured by loading ER with fluo-5N and then washing dye from the cytoplasm with a dye-free patch pipette solution. Small dye molecules diffused within ER between soma and terminal showing a single continuous ER compartment. Depolarization of rods to −40 mV depleted Ca^{2+} from terminal ER, followed by a decline in somatic ER $[Ca^{2+}]$. Local activation of ryanodine receptors in terminals with a spatially confined puff of ryanodine caused a decline in terminal ER $[Ca^{2+}]$, followed by a secondary decrease in somatic ER. Localized photolytic uncaging of Ca^{2+} from *o*-nitrophenyl-EGTA in somatic ER caused an abrupt Ca^{2+} increase in somatic ER, followed by a slower Ca^{2+} increase in terminal ER. These data suggest that, during maintained depolarization, a soma-to-terminal $[Ca^{2+}]$ gradient develops within the ER that promotes diffusion of Ca^{2+} ions to resupply intraterminal ER Ca^{2+} stores and thus sustain CICR-mediated synaptic release. The ability of Ca^{2+} to move freely through the ER may also promote bidirectional communication of Ca^{2+} changes between soma and terminal.

Key words: calcium imaging; calcium-induced calcium release; endoplasmic reticulum; retina; rod photoreceptors; synaptic terminal

Significance Statement

Vertebrate rod and cone photoreceptors both release vesicles at synaptic ribbons, but rods also exhibit substantial slow release at non-ribbon sites triggered by Ca^{2+}-induced Ca^{2+} release (CICR). Blocking CICR inhibits >50% of release from rods in darkness. How do rods maintain sufficiently high $[Ca^{2+}]$ in terminal endoplasmic reticulum (ER) to support sustained CICR-driven synaptic transmission? We show that maintained depolarization creates a $[Ca^{2+}]$ gradient within the rod ER lumen that promotes soma-to-terminal diffusion of Ca^{2+} to replenish intraterminal ER stores. This mechanism allows CICR-triggered synaptic release to be sustained indefinitely while rods remain depolarized in darkness. Free diffusion of Ca^{2+} within the ER may also communicate synaptic Ca^{2+} changes back to the soma to influence other critical cell processes.

Introduction

Vertebrate photoreceptors transmit light-evoked voltage changes to second-order retinal neurons by changing glutamate release rates. Rods and cones both exhibit fast ribbon-mediated release of vesicles, but slow sustained release from rods also involves significant release at non-ribbon sites (Snellman et al., 2011; Chen et al., 2013, 2014). This slow non-ribbon release contributes to slower release kinetics in rods versus cones, paralleling the slower light response kinetics of rods (Schnapf and Copenhagen, 1982; Cadetti et al., 2005; Rabl et al., 2005). In amphibian and mammalian retinas, slow, non-ribbon release from rods is triggered by Ca^{2+}-induced Ca^{2+} release (CICR) into cytoplasm

Received Feb. 23, 2015; revised June 8, 2015; accepted July 6, 2015.

Author contributions: M.C. and W.B.T. designed research; M.C., M.J.V.H., and W.B.T. performed research; M.C., M.J.V.H., and W.B.T. analyzed data; M.C. and W.B.T. wrote the paper.

This research was supported by National Institutes of Health Grants R01EY10542 (W.B.T.) and F32EY023864 (M.J.V.H.), a Senior Scientific Investigator Award from Research to Prevent Blindness (W.B.T.), and a University of Nebraska Medical Center Graduate Fellowship (M.C.).

The authors declare no competing financial interests.

Correspondence should be addressed to Dr. Wallace B. Thoreson, Department of Ophthalmology and Visual Sciences, University of Nebraska Medical Center, 4050 Durham Research Center I, Omaha, NE 68198-5840. E-mail: wbthores@unmc.edu.

DOI:10.1523/JNEUROSCI.0754-15.2015

 0270-6474/15/3511364-10$15.00/0

from endoplasmic reticulum (ER) stores (Krizaj et al., 1999, 2003; Cadetti et al., 2006; Suryanarayanan and Slaughter, 2006; Babai et al., 2010; Chen et al., 2014). Blocking CICR in mouse and salamander retina inhibits rod-driven light responses of second-order neurons by 50–90%, indicating that CICR is a major mechanism for maintaining high cytoplasmic [Ca^{2+}] needed to sustain vesicle release from rods in darkness (Cadetti et al., 2006; Suryanarayanan and Slaughter, 2006; Babai et al., 2010). Ca^{2+} exits ER during CICR in rods through ryanodine receptors (RyRs); immunohistochemical studies show the presence of RyRs but not inositol 1,4,5-trisphosphate receptors in rod terminals (Krizaj et al., 2003, 2004). The principal RyR subtype in rods is a RyR2 splice variant (Shoshan-Barmatz et al., 2005, 2007).

How can CICR contribute indefinitely to elevation of Ca^{2+} in rod terminals without exhausting intraterminal ER Ca^{2+} stores? ER appears to be present in somas, axons, and terminals of rods from most, if not all, vertebrates (De Robertis and Franchi, 1956; De Robertis, 1956; Ladman, 1958; Ungar et al., 1981; Mercurio and Holtzman, 1982; Freihöfer et al., 1990; Johnson et al., 2007; Babai et al., 2010; Chen et al., 2014). Immunohistochemical labeling for sarco/ER Ca^{2+} ATPase type 2 (SERCA2) partially colocalizes with labeling for the ribbon protein Ribeye in mouse retina, supporting ultrastructural evidence that ER approaches close to ribbons (Babai et al., 2010). Fluorescence loss in photobleaching (FLIP) and other approaches indicate that the ER forms a continuous structure in many cells (Dayel et al., 1999; Park et al., 2000; Estrada de Martin et al., 2005; Verkhratsky, 2005). Similarly, fluorescence recovery after photobleaching (FRAP) experiments with ER-tracker dye suggested that the ER in salamander rods extends continuously from soma to terminal (Chen et al., 2014). Ca^{2+} accumulates within ER of rods, attaining especially high levels in somatic ER (Ungar et al., 1981; Somlyo and Walz, 1985). In other cell types, Ca^{2+} ions have been shown to diffuse within the ER from one region of a cell to another (Mogami et al., 1997; Park et al., 2000; Choi et al., 2006; Wu and Bers, 2006; Petersen and Verkhratsky, 2007; Swietach et al., 2008; Picht et al., 2011; Bers and Shannon, 2013). Experiments described in the present study showed that lengthy depolarization of salamander rods causes a sustained decline in somatic ER [Ca^{2+}] without causing a substantial increase in cytoplasmic [Ca^{2+}] of the soma. We hypothesized that Ca^{2+} depleted from rod terminal ER stores during sustained depolarization can be replenished by diffusion of Ca^{2+} through the ER lumen from reservoirs in the axon and soma. To test this idea, we combined use of ER and cytoplasmic Ca^{2+} dyes with various techniques, including FRAP, FLIP, voltage clamp, flash photolysis of caged Ca^{2+}, and localized activation of RyRs. The results showed that activation of CICR during sustained depolarization of rods generates a soma-to-terminal [Ca^{2+}] gradient within the ER, promoting diffusion of Ca^{2+} through the ER from the perikaryon to resupply Ca^{2+} stores in the synaptic terminal. This nearly inexhaustible mechanism for sustaining CICR helps to maintain high Ca^{2+} levels necessary for sustaining synaptic release from rods as they remain depolarized in darkness. Free Ca^{2+} diffusion through the ER may also communicate synaptic Ca^{2+} changes back to the soma, which can influence mitochondrial function, stress responses, or other processes.

Materials and Methods

Animal care and use. Both sexes of aquatic tiger salamanders (*Ambystoma tigrinum*, 18–25 cm in length; Charles Sullivan) were used for experiments. They were maintained on a 12 h light/dark cycle and killed 1–2 h after the beginning of the dark cycle. Salamanders were anesthetized by bathing with MS-222 (0.25 g/L) for 30 min before being decapitated with heavy shears. The head was hemisected and the spinal cord pithed. Protocols were approved by the University of Nebraska Medical Center Institutional Animal Care and Use Committee.

Photoreceptor isolation. Details of the photoreceptor isolation procedures have been described previously (Chen et al., 2013). Briefly, retinas were digested by incubation with papain (30 U/ml; Worthington) plus cysteine (0.2 mg/ml) in Ca^{2+}-free amphibian saline solution containing the following (in mM): 116 NaCl, 2.5 KCl, 5 $MgCl_2$, 10 HEPES, and 5 glucose, pH 7.4 (for 35 min at room temperature). The tissue was then washed in ice-cold, Ca^{2+}-free amphibian saline containing 1% bovine serum albumin and deoxyribonuclease I (1 mg/ml; Worthington), followed by two additional washes in ice-cold, Ca^{2+}-free saline. A piece of retina was triturated with a fire-polished Pasteur pipette, and the cell suspension was transferred onto glass slides or 1.78 refractive index coverslips (Olympus) coated with Cell-Tak (3.5 $\mu g/cm^2$; BD Biosciences). After letting cells settle and adhere for 30 min at 4°C, they were superfused with oxygenated amphibian saline solution containing the following (in mM): 116 NaCl, 2.5 KCl, 1.8 $CaCl_2$, 0.5 $MgCl_2$, 10 HEPES, and 5 glucose, pH 7.8 (at room temperature). Ca^{2+} dyes were obtained from Invitrogen (Life Technologies). Unless otherwise specified, other reagents were obtained from Sigma-Aldrich. Rods were identified by their characteristic morphology including an axon and round or tear drop-shaped terminals. Intact terminals in retinal slices typically have a diameter of ~5 μm. The terminals of isolated rods tended to flatten out against the coverslip to a thickness of 1–2 μm. Light-sensitive outer segments of rods were typically lost during trituration.

Imaging. For FRAP, FLIP, and confined ryanodine puff experiments, isolated rods were studied on an inverted microscope (Olympus IX71) by either total internal reflection fluorescence (TIRF) or epifluorescence. For TIRF measurements of Ca^{2+} indicator dyes, a 488 nm solid-state laser (Melles Griot) was focused off-axis onto the back focal plane of a 1.65 numerical aperture (NA) objective (Apo 100× oil; Olympus). After leaving the objective, light traveled through a high refractive index (1.78) immersion fluid (Cargille Laboratories) and entered the coverslip, undergoing total internal reflection at the interface between the glass and lower refractive index of the cell membrane or overlying aqueous medium. The evanescent wave propagated at this interface had a length constant of 57 nm (Chen et al., 2013). Fluorescence emission was filtered by a 525 nm (45-nm-wide) bandpass filter (Semrock). For epifluorescence measurements, we used a 60×, 1.45 NA oil-immersion objective, illuminated isolated rods with 467–498 nm excitation light from a 120 W mercury lamp (XCite 120Q; Olympus), and collected the emitted fluorescence at 513–556 nm. Imaging data for both TIRF and epifluorescence experiments were acquired through an EMCCD camera (Hamamatsu ImageEM) at 31 ms/frame using MetaMorph software (Molecular Devices) and analyzed with MetaMorph or NIH ImageJ 1.46.

For monitoring Ca^{2+} changes during lengthy depolarizing steps applied to voltage-clamped rods or flash photolysis of caged Ca^{2+} compounds, fluorescence from Ca^{2+} dyes was collected through a 60×, 1.0 NA, water-immersion objective on an upright fixed-stage microscope (Nikon E600FN) equipped with a spinning-disk confocal scan head (Ultraview LC; PerkinElmer Life and Analytical Sciences). Excitation light at 488 or 568 nm was delivered from an argon/krypton laser, and emission was collected at 525 or 600 nm, respectively, by a cooled CCD camera (Hamamatsu OrcaER). Images were acquired and analyzed using PerkinElmer Imaging Suite version 5.5.

Retinal slice preparation and electrophysiology. We used retinal slice preparations for some experiments. Details of slice preparation and electrophysiological recordings have been described previously (Van Hook and Thoreson, 2013). To monitor [Ca^{2+}] changes in the cytoplasm and ER simultaneously during sustained depolarization, we loaded the ER with a low-affinity Ca^{2+} indicator dye, fluo-5N AM (K_d of 90 μM) and monitored cytoplasmic changes with a higher-affinity dye, rhod-2 (K_d of 570 nM), introduced through a whole-cell patch pipette. First, retinal slices (125 μm thick) were incubated with fluo-5N AM (10 μM) for 2.5 h at 4°C to load dye into both cytoplasm and ER. Retinal slices were then placed on the upright fixed-stage microscope and superfused with oxygenated amphibian saline. Rods were voltage clamped using an Axopatch

200B (Molecular Devices) patch-clamp amplifier. Currents were acquired and analyzed using pClamp 9.2 software with Digidata 1322 interface (Molecular Devices). Cells with holding currents >300 pA were excluded from analysis.

Recording pipettes were pulled on a PP-830 vertical puller (Narishige International) from borosilicate glass pipettes (1.2 mm outer diameter, 0.9 mm inner diameter, with internal filament; World Precision Instruments). Pipette resistance was 12–18 MΩ. Rod pipettes were filled with the following (in mM): 40 cesium glutamate, 50 cesium gluconate, 9.4 tetraethylammonium-Cl, 3.5 NaCl, 1 $MgCl_2$, 9.4 MgATP, 0.5 GTP, 5 EGTA, 10 HEPES, and 0.1 rhod-2 tripotassium salt, pH 7.2. After obtaining the whole-cell recording configuration, fluo-5N was washed out of the cytoplasm but remained in the ER (Solovyova and Verkhratsky, 2002). At the same time, the higher-affinity rhod-2 was introduced into the cytoplasm through the patch pipette. We waited at least 5 min to wash fluo-5N completely out of the cytoplasm. In experiments in which we measured ER Ca^{2+} changes without measuring cytoplasmic Ca^{2+}, we omitted rhod-2 from the pipette solution. Rods were depolarized for 17 s from −70 to −40 mV, similar to the photoreceptor membrane potential in darkness. rhod-2 and fluo-5N were alternately illuminated by 568 and 488 nm light, respectively. With 488 nm excitation/525 nm emission, rhod-2 fluorescence was 10.8% of the intensity observed with 568 nm excitation/600 nm emission. Therefore, we corrected fluo-5N fluorescence collected at 600 nm for bleed-through from rhod-2 fluorescence by subtracting a 10.8% scaled version of the rhod-2 fluorescence. There was no detectable fluo-5N fluorescence observed in the rhod-2 channel.

FRAP and FLIP experiments. To examine Ca^{2+} diffusion within ER, we loaded the ER of isolated rods with fluo-5N as described above for retinal slices. Isolated rods were incubated with fluo-5N AM (10 μM) for 1 h at 4°C to load dye into the cytoplasm and ER. After loading, we obtained whole-cell patch-clamp recordings using a Ca^{2+}- and dye-free pipette solution to wash dye out of the cytoplasm. To examine FRAP with cytoplasmic dye, we loaded rods with a high-affinity Ca^{2+} indicator by incubating cells with fluo-4 AM for 30 min at 4°C. In FRAP and FLIP experiments, terminals or somas of rods were photobleached for 1–4 s by illumination with a small spot (5–8 μm diameter) from a 30 mW, 488 nm laser. Loss and recovery of fluo-5N or fluo-4 fluorescence were monitored by epifluorescence.

The epifluorescent measurement light used to monitor fluorescence recovery sometimes produced additional photobleaching during the recovery phase. To compensate for bleaching by the epifluorescent measurement light, we measured fluorescence declines in somas of neighboring cells that were not photobleached by the laser spot and fit fluorescence declines in those cells with an exponential function. In rods loaded with fluo-5N that were subject to laser photobleaching, fitting data from only the 2 s period before laser photobleach yielded a fluorescence decline attributable to the epifluorescent measurement light of 15.5% in 12.5 s, with a time constant (τ) of 16 s. The decline in soma fluorescence measured throughout the entire trial in neighboring rods that were not photobleached by the laser exhibited a similar rate of bleaching by the epifluorescent measurement light (15% in 12.5 s; $\tau = 18$ s). During FLIP experiments, we used weaker epifluorescent illumination that did not produce noticeable bleaching.

Depletion of Ca^{2+} in terminal ER by confined puff application of ryanodine. To activate RyRs and thus stimulate CICR in the terminal of isolated rods, we used a spatially confined pressure ejection (Toohey) of ryanodine (30–100 μM) applied to terminals for 200 to 500 ms. Ryanodine promotes opening of RyRs at low micromolar concentrations (1–10 μM) but blocks RyRs at high micromolar concentrations (50–100 μM). However, the short puff duration reduced its effective concentration so that ryanodine puffs acted as RyR agonists. The tip of the puffer pipette was positioned ~3 μm away from the terminal. At the terminal, the diameter of the puff expanded to 6–7.2 μm as measured with fluorescein puffs. To monitor $[Ca^{2+}]$ changes in the cytoplasm, we loaded isolated rods with fluo-5F AM (10 μM, K_d of 2.3 μM) at 4°C for 30 min. To monitor $[Ca^{2+}]$ changes in ER, we loaded isolated rods with fluo-5N AM for 1 h and obtained whole-cell recordings with a dye-free pipette solution to wash away cytoplasmic dye as described above.

Elevation of Ca^{2+} by localized photolysis of o-nitrophenyl-EGTA. To examine diffusion of Ca^{2+} in the cytoplasm and ER, we used a caged Ca^{2+} compound, *o*-nitrophenyl (NP)-EGTA (Invitrogen). K_d of NP-EGTA for Ca^{2+} increases from 80 to >1 mM during UV illumination. Chelated Ca^{2+} was released by a 1.5 ms UV light flash from a xenon arc flash lamp (JML-C2 Flash Lamp System; Rapp OptoElectronic) with a diameter of 6 μm and centered on the rod soma.

To examine diffusion of Ca^{2+} in the cytoplasm of isolated rods, cells were incubated with NP-EGTA AM (10 μM) and fluo-4 AM (10 μM) for 45 min at 4°C. In one set of experiments, retinal slices were incubated with NP-EGTA AM (10 μM), and then rods were voltage clamped with a pipette solution containing Oregon Green BAPTA-6F (OGB-6F; 500 μM) and ryanodine (2 μM). In recordings from slices, we used OGB-6F because it exhibits higher basal fluorescence than fluo-5F, making it easier to see rod terminals under confocal microscopy. Ryanodine was included in the pipette to stimulate the opening of RyR channels.

To examine diffusion of Ca^{2+} within the ER lumen, isolated rods were incubated with NP-EGTA AM (10 μM) and fluo-5N AM (10 μM) for 2.5 h at 4°C. For measurements of ER Ca^{2+} changes in these experiments, NP-EGTA and fluo-5N in cytoplasm were washed out of the cytoplasm by introducing dye-free intracellular solution through patch pipettes. To confirm that NP-EGTA was washed away completely from cytoplasm, we conducted control experiments in which we loaded ER with NP-EGTA and then introduced membrane-impermeant fluo-5F pentapotassium salt (100 μM) through the patch pipette to monitor $[Ca^{2+}]$ changes in the cytoplasm. We also conducted similar control experiments in rods from retinal slices using the dye OGB-6F (500 μM) after loading the ER with NP-EGTA-AM.

Statistical analysis. We performed statistical analysis using GraphPad Prism 4. Results are presented as mean ± SEM, and statistical significance was determined using Student's *t* test. When comparing experiments involving multiple measurements (see Fig. 2), we compared the average of five data points from each cell in both conditions. We chose $p < 0.05$ to be the criterion for statistical significance.

Results

ER lumen is continuous from soma to terminal

ER appears to be present in the cell bodies, axons, and terminals of all vertebrate rods that have been examined, including rat, mouse, rabbit, frog, salamander, and teleost fish (De Robertis and Franchi, 1956; De Robertis, 1956; Ladman, 1958; Ungar et al., 1981; Mercurio and Holtzman, 1982; Freihöfer et al., 1990; Johnson et al., 2007; Babai et al., 2010). FRAP experiments using ER-tracker green dye that labels K^+ channels in the ER membrane showed that the ER membrane in rods is continuous from terminal to soma (Chen et al., 2014). To test whether small molecules can diffuse within the ER lumen from soma to terminal, we loaded ER in isolated rods with a low-affinity Ca^{2+} indicator fluo-5N (K_d of 90 μM). We selected this dye because it can report the high levels of Ca^{2+} that are present in the ER (60–1000 μM; Bygrave and Benedetti, 1996; Michalak et al., 2002; Solovyova and Verkhratsky, 2002). After loading cells with fluo-5N AM, we obtained whole-cell patch-clamp recordings using a Ca^{2+}- and dye-free pipette solution to wash fluo-5N out of the cytoplasm, leaving it within the ER lumen (Solovyova and Verkhratsky, 2002; Chen et al., 2014). After waiting for 5 min after patch rupture, depolarizing voltage steps caused intraterminal fluo-5N fluorescence to decrease (Chen et al., 2014). This depolarization-evoked decline in fluo-5N fluorescence showed that Ca^{2+} leaves the ER during activation of CICR and confirmed that Ca^{2+} dye was washed out of the cytoplasm (Chen et al., 2014).

As shown in Figure 1*A*, isolated rods were incubated with fluo-5N AM for 1 h and then patched with a dye-free pipette solution to wash dye out of the cytoplasm but not the ER. Axonal ER is very thin, and so its fluorescence is very faint. We bleached the terminal

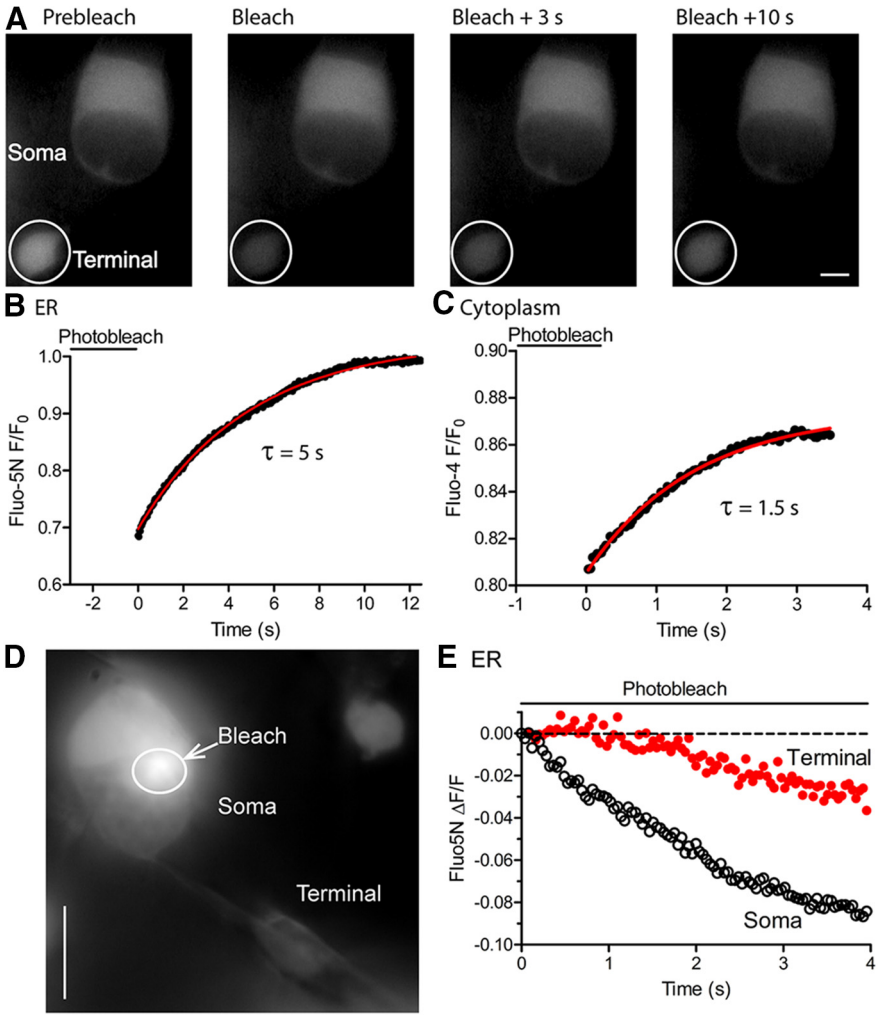

Figure 1. FRAP and FLIP experiments show that ER lumen is continuous from soma to terminal. ***A***, Series of epifluorescence images from an isolated rod in which the ER was loaded with fluo-5N and the dye was washed out of the cytoplasm during whole-cell recording. The images show fluo-5N fluorescence before and after photobleaching the synaptic terminal with a 488 nm laser spot of 8 μm in diameter (white circle). The strong fluorescence in the inner segment is primarily attributable to autofluorescence of mitochondrial flavonoids. Scale bar, 2 μm. ***B***, The time course for FRAP of fluo-5N fluorescence (F/F_0) in the same rod terminal. F_0 is the average fluorescence intensity in the terminal before bleaching. As described in Materials and Methods, bleaching by the epifluorescent measurement light during the recovery phase was estimated and corrected with an exponential decay function. The red curve shows an exponential fit to the corrected rate of fluorescence recovery ($\tau = 5$ s). Photobleaching lasted 3 s, and recovery of fluorescence was recorded from time 0 at 31.3 ms/frame. ***C***, The time course for recovery of cytosolic fluo-4 fluorescence (F/F_0) in another rod terminal after photobleaching with a 488 nm laser spot (filled circles). The red curve shows an exponential fit to the rate of fluorescence recovery after correcting for bleaching by the epifluorescent measurement light ($\tau = 1.5$ s). ***D***, Epifluorescence image of an isolated rod loaded with fluo-5N and then patch clamped to wash dye out of the cytosol. The image shows the cell during photobleach of fluo-5N fluorescence with a 488 nm spot positioned over the soma (circle). Scale bar, 5 μm. ***E***, FLIP in terminal ER (red filled circles) was delayed relative to fluorescence loss in soma ER during laser photobleach (black open circles). In this experiment, it was not necessary to correct for photobleaching by the epifluorescent measurement light.

using a spatially confined laser spot (488 nm, 30 mW, 8 μm in diameter; Fig. 1*A*, white circle) applied for 3 s while monitoring changes in fluo-5N fluorescence. Rod terminals that were photobleached showed almost complete recovery of fluorescence (Fig. 1*B*). Bleaching by the epifluorescent measurement light during the recovery phase was estimated and corrected with an exponential decay function (see Materials and Methods). After correction, the time constant of fluorescence recovery in the terminal averaged 6.3 ± 0.95 s ($n = 8$; Table 1).

We also conducted FRAP experiments to examine diffusion of dye through the cytoplasm. For these experiments, we used a higher-affinity dye (fluo-4 AM), loaded rods for only 30 min to preferentially load cytoplasm, and did not voltage clamp the cells. After laser photobleach of terminal fluorescence for 1–3 s, partial recovery of cytoplasmic fluorescence was observed (Fig. 1*C*) that averaged $\tau = 2.3 \pm 0.54$ s ($n = 5$; Table 1). This is approximately threefold faster than FRAP of fluo-5N in the ER. The rapid kinetics of cytoplasmic recovery suggests that dye diffused back into the terminal during the 1–3 s bleaching period. Rapid return of dye during the photobleach period would explain the modest bleaching produced by the laser. Bleaching of additional returning dye would also explain why there was only partial recovery of fluorescence after the bleaching period. The faster recovery of fluorescence in the cytoplasm compared with ER is presumably attributable to a lower degree of tortuosity.

Additional confirmation of continuity between soma and terminal ER was provided by FLIP experiments. As in Figure 1*A–C*, we loaded isolated rods with fluo-5N for 1 h and then patch clamped them to wash dye out of the cytoplasm. We bleached dye in a local region of somatic ER by applying a 488 nm laser spot (5 μm; Fig. 1*D*,*E*). In the example shown in Figure 1, fluorescence declined in the bleached area with a time constant of 2 s. Fluorescence also declined in the unbleached terminal, and this fluorescence loss was delayed with respect to that of the soma (Fig. 1*D*,*E*), consistent with dye diffusion from terminal to soma during the photobleach period. Similar delayed FLIP of terminal ER fluorescence was observed while photobleaching the somas of eight rods. In summary, FRAP and FLIP experiments showed that small molecules can move freely between the soma and terminal within the ER lumen.

Depletion of terminal ER Ca^{2+} during long depolarizing steps reduced somatic ER Ca^{2+}

In darkness, rods have a resting membrane potential of approximately −40 mV, stimulating the opening of voltage-gated Ca^{2+} channels in the terminal. The influx of Ca^{2+} through open Ca^{2+} channels in turn activates CICR in the terminal. The ability of rods to release glutamate-filled vesicles continuously in darkness indicates that intraterminal $[Ca^{2+}]$ must remain elevated indefinitely. To determine whether this sustained elevation of intraterminal $[Ca^{2+}]$ involves sustained activation of CICR, we loaded rods with both fluo-5N in the ER and rhod-2 in the cytoplasm to examine Ca^{2+} changes in the two cell compartments simultaneously. The low-affinity Ca^{2+} indicator fluo-5N AM was loaded into ER and cytoplasm by incubating retinal slices with the dye. Rods were then patched with a pipette containing rhod-2 (100 μM) to wash fluo-5N out of the cytoplasm and replace it with rhod-2 (Fig. 2*A*). $[Ca^{2+}]$ changes in ER and cytoplasm were then monitored by alternately measuring

Table 1. Kinetics of diffusion in cytoplasm and ER

	Diffusion coefficient of Ca^{2+} ions ($\mu m^2/s$)	Time constant of fluorescence recovery (s)
Cytoplasm	32.6 ± 7.3 ($n = 8$)	fluo-4, 2.3 ± 0.54 ($n = 5$)
ER	23.1 ± 2.9 ($n = 14$)	fluo-5N, 6.3 ± 0.95 ($n = 8$)
Mixed[a]	30.6 ± 4.1 ($n = 5$)	

[a]Uncaged Ca^{2+} in somatic ER with open RyRs.

fluo-5N fluorescence with a 488 nm laser and rhod-2 fluorescence with a 568 nm laser on a spinning-disk confocal microscope. Cytoplasmic rhod-2 fluorescence increased slowly in the terminal during a 17 s depolarizing step from −70 to −40 mV ($p = 0.013$, $n = 6$; Fig. 2*B*, red), attaining a plateau after ~12 s. At the same time, fluo-5N fluorescence in terminal ER declined ($p = 0.04$, $n = 6$; Fig. 2*C*, red), showing a progressive depletion of Ca^{2+} stores that also appeared to plateau after 12 s. The parallel between the rise in cytoplasmic Ca^{2+} and decline in ER Ca^{2+} suggests that the rise in cytoplasmic Ca^{2+} was not only attributable to Ca^{2+} influx through membrane Ca^{2+} channels but also involved continued Ca^{2+} release from ER stores.

Similar to the terminal, cytoplasmic [Ca^{2+}] also rose in the soma ($p = 0.004$, $n = 6$; Fig. 2*B*, black) whereas ER [Ca^{2+}] declined ($p = 0.0008$, $n = 6$; Fig. 2*C*, black) during sustained depolarization. However, the depolarization-evoked increase in cytoplasmic [Ca^{2+}] in the soma was only ~3% of the cytoplasmic [Ca^{2+}] increase observed in the terminal, as measured by $\Delta F/F$ with rhod-2 ($p = 0.004$, $n = 6$; Fig. 2*B*, black). In comparison, the decline in somatic ER [Ca^{2+}] measured with fluo-5N (Fig. 2*C*, black) was a larger fraction (~25%) of the decline in terminal ER [Ca^{2+}] ($n = 6$). The decline in terminal ER [Ca^{2+}] also appeared larger than the decline in somatic ER [Ca^{2+}], although the difference did not attain statistical significance ($p = 0.12$). Although differing dye Ca^{2+} affinities and differences in the volumes of ER and cytoplasm make precise quantitative comparisons difficult, the 3% increase in cytoplasmic $\Delta F/F$ observed with rhod-2 (K_d of 570 nM) is likely to involve a smaller Ca^{2+} change than the 25% decrease in ER $\Delta F/F$ observed with the much lower-affinity dye fluo-5N (K_d of 90 μM). This suggests that not all of the Ca^{2+} ions that leave the somatic ER enter the surrounding cytoplasm, but instead some of them diffuse through ER to the terminal. In addition to release of Ca^{2+} from somatic ER, the rise of cytoplasmic [Ca^{2+}] in the soma might also involve diffusion of Ca^{2+} through the cytoplasm from the terminal or entry of Ca^{2+} through membrane channels in the soma (e.g., L-type Ca^{2+} channels or store-operated channels). The evidence for smaller ER [Ca^{2+}] declines in the soma than in the terminal suggests that, with maintained depolarization, a gradient of [Ca^{2+}] develops within the ER, with higher levels in the soma and lower levels in the terminal. This concentration gradient would help to drive diffusion of Ca^{2+} through the ER from soma to terminal and thereby help to sustain CICR in the terminal during maintained depolarization.

Decreasing terminal ER Ca^{2+} caused a secondary decrease in somatic ER Ca^{2+}

To test further whether Ca^{2+} can diffuse from soma to terminal within the ER, we depleted Ca^{2+} locally from intraterminal ER by applying spatially confined puffs of ryanodine (30–100 μM, 6–7.5 μm diameter) to terminals of isolated rods. To test whether ryanodine puffs could activate terminal RyRs without also activating RyRs in the soma, we loaded isolated rods with a Ca^{2+} indicator fluo-5F (K_d of 2.3 μM) to monitor cytoplasmic [Ca^{2+}]

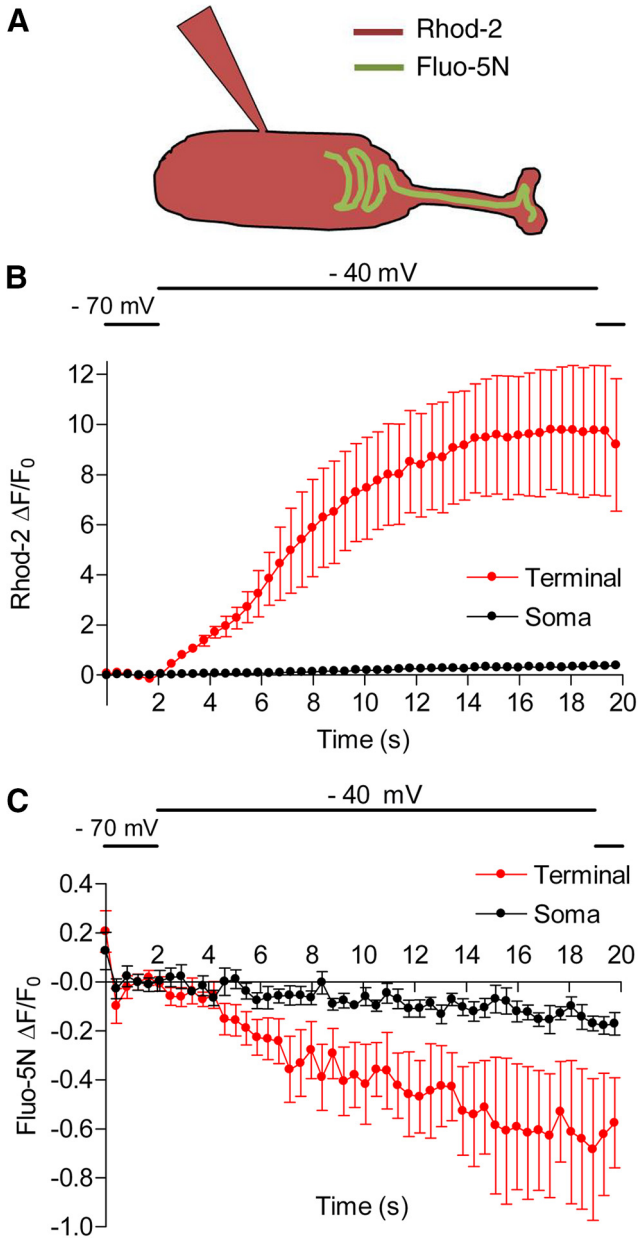

Figure 2. Depletion of terminal ER Ca^{2+} stores during long depolarizing steps led to a decline in [Ca^{2+}] in somatic ER. ***A***, Diagram illustrates loading of fluo-5N and rhod-2 into ER and cytoplasm, respectively. A low-affinity Ca^{2+} indicator, fluo-5N AM, was loaded into cytoplasm and ER of photoreceptors by incubating retinal slices with the dye for 2.5 h. Photoreceptors were then patched with a pipette containing rhod-2 (100 μM) without fluo-5N to remove fluo-5N from the cytoplasm and replace it with rhod-2. [Ca^{2+}] changes in ER and cytoplasm were monitored alternately by illuminating fluo-5N in the ER with 488 nm laser light and illuminating rhod-2 in the cytoplasm with 568 nm laser light using a spinning-disk confocal microscope. The time interval between image pairs was 420 ms. ***B***, rhod-2 fluorescence changes showed a slow increase in terminal cytoplasmic [Ca^{2+}] (red) during a depolarizing step from −70 to −40 mV for 17 s. Cytoplasmic [Ca^{2+}] in the soma (black) increased by only a very small amount during that time. ***C***, fluo-5N fluorescence changes showed that terminal ER [Ca^{2+}] (red) decreased during 17 s depolarizing steps. Somatic ER [Ca^{2+}] (black) showed a smaller decline. The graphs in ***B*** and ***C*** show the average ± SEM from six rods.

changes (Fig. 3*A*,*B*). We then puffed ryanodine (30–100 μM) onto the terminal (Fig. 3*A*) or soma (Fig. 3*B*) for 200–500 ms. Use of a short puff duration reduced its effective concentration so that ryanodine acted as an agonist at RyRs. In most cells, puffing ryanodine (30–100 μM) directly onto terminals stimulated an elevation of terminal cytoplasmic [Ca^{2+}] (30 μM, 9 of 12; 100

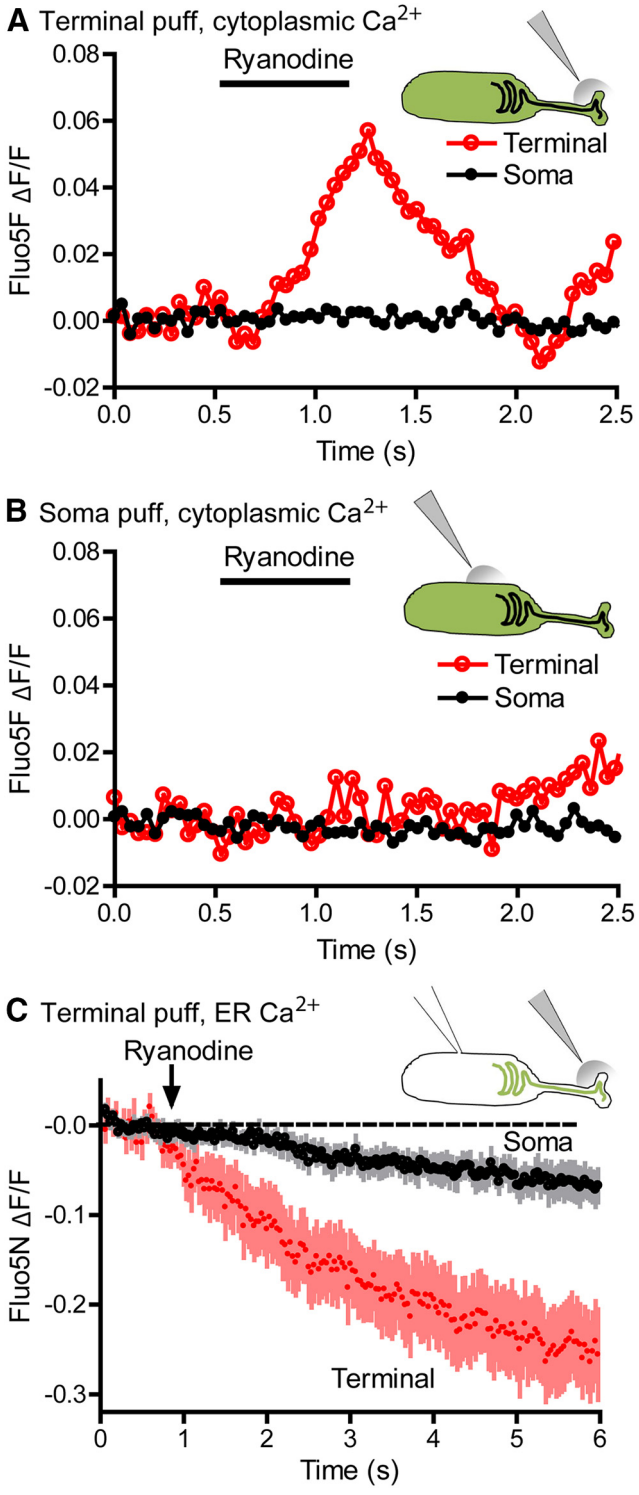

Figure 3. Depletion of terminal ER Ca^{2+} stores stimulated by opening of terminal RyRs was followed by a secondary decline in somatic ER $[Ca^{2+}]$. ***A***, Application of a spatially confined puff of ryanodine (100 μM, 0.5 s) to the terminal of an isolated rod stimulated an increase in cytoplasmic Ca^{2+} in the terminal (open red circles) but not the soma (filled black circles). ***B***, Puffing ryanodine onto the soma of the same rod caused no Ca^{2+} change in either terminal (open red circles) or somatic cytoplasm (filled black circles). For experiments in ***A*** and ***B***, isolated rods were loaded with the Ca^{2+} indicator fluo-5F to visualize cytoplasmic $[Ca^{2+}]$ changes on an inverted microscope by epifluorescence. ***C***, Average ± SEM data from eight rods shows that puffing ryanodine (100 μM, 200–500 ms) onto rod terminals caused Ca^{2+} to decline in both terminal (red) and somatic ER (black). For experiments in ***C***, isolated rods were loaded with a low-affinity Ca^{2+} indicator fluo-5N (K_d of 90 μM), and then dye was washed out of the cytoplasm by introducing a dye-free intracellular solution through a patch pipette. Submembrane Ca^{2+} changes in the ER of isolated rods were then visualized by TIRF microscopy. Insets illustrate the experimental configurations.

μM, 17 of 23 cells; Fig. 3*A*, open red circles), consistent with release of Ca^{2+} from ER. Typically, there was no change in somatic $[Ca^{2+}]$ after a puff onto the terminal (Fig. 3*B*, filled black circles), although in some cells we observed a small cytoplasmic $[Ca^{2+}]$ increase in the soma (data not shown). The small increase in somatic $[Ca^{2+}]$ in these cells was probably secondary to intracellular diffusion of Ca^{2+} from the terminal because direct application of ryanodine puffs to the soma did not stimulate Ca^{2+} increases in the soma (Fig. 3*B*) regardless of whether puffs were applied before (100 μM, 0 of 14 cells) or after (30 μM, 0 of 3 cells; 100 μM, 0 of 9 cells) puffs to the terminal. Although puffing ryanodine onto the soma did not stimulate increases in somatic $[Ca^{2+}]$, on a few occasions, puffing ryanodine onto the soma stimulated intraterminal $[Ca^{2+}]$ increases (30 μM, 0 of 3 cells; 100 μM, 3 of 23 cells). These data indicate that Ca^{2+} release can be stimulated more easily in the terminal than soma and show that confined puffs to the terminal can directly activate RyRs in that compartment.

Next, we measured Ca^{2+} changes in the ER by incubating cells with fluo-5N AM (K_d of 90 μM) and then washing dye out of the cytoplasm by introducing a dye-free solution into the rod through a patch pipette (Fig. 3*C*). We found that ER $[Ca^{2+}]$ decreased within the terminal after a localized ryanodine puff to the terminal (normalized $\Delta F/F = -0.25 \pm 0.046$, $p = 0.0006$, $n = 8$), consistent with release of Ca^{2+} from ER to cytoplasm by activation of RyRs. Localized activation of RyR-mediated Ca^{2+} release in the terminal also caused a secondary decline in somatic ER $[Ca^{2+}]$ (normalized $\Delta F/F = -0.064 \pm 0.018$, $p = 0.0033$, $n = 8$). The decline in somatic $[Ca^{2+}]$ developed more slowly than the decline in intraterminal $[Ca^{2+}]$, consistent with the possibility that it resulted from diffusion of Ca^{2+} through the ER from soma to terminal. The decline in the soma was smaller than that in the terminal ($p = 0.0058$, $n = 8$), consistent with a larger Ca^{2+} store in the soma than the terminal. Figure 3*C* shows average data from eight cells visualized by TIRF microscopy. When we measured fluo-5N fluorescence changes using epifluorescent illumination, the $\Delta F/F$ changes were smaller (-0.036 ± 0.013, $n = 6$, $p = 0.0018$ compared with fluorescence changes monitored by TIRF), suggesting that spatially averaged changes are smaller than local submembrane changes in ER Ca^{2+}. The finding that depletion of terminal ER Ca^{2+} is followed by a delayed decline in somatic ER Ca^{2+} supports the hypothesis that terminal and somatic ER form a single interconnected Ca^{2+} store in rod photoreceptors.

Increasing somatic ER Ca^{2+} caused a secondary rise in terminal ER Ca^{2+}

We also tested interconnectedness of the ER lumen by determining whether increasing $[Ca^{2+}]$ in somatic ER causes a secondary increase in terminal ER. To do so, we loaded the ER with a caged Ca^{2+} compound, NP-EGTA, that releases Ca^{2+} during photolysis by UV light. We then flashed a small spot (6 μm diameter) of UV light onto the soma to uncage Ca^{2+} only in the soma. To load the ER with NP-EGTA, we incubated rods with NP-EGTA AM for 2.5 h and then washed NP-EGTA out of the cytoplasm by introducing a drug-free solution into the cell through a whole-cell patch pipette. To test whether NP-EGTA was successfully washed out of the cytoplasm, we

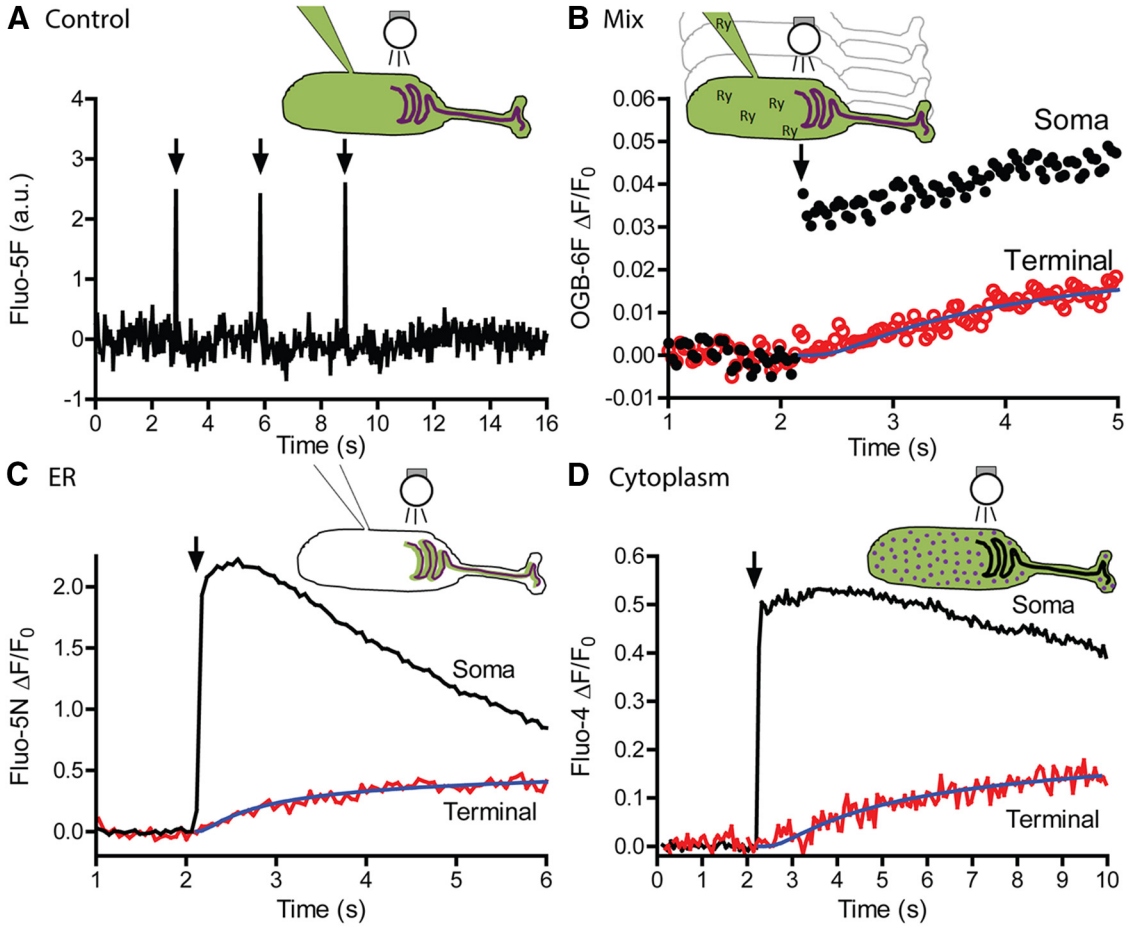

Figure 4. Photolytic uncaging of Ca^{2+} from NP-EGTA within somatic ER triggered a secondary slow increase in terminal ER $[Ca^{2+}]$. ***A***, Control experiment demonstrating that the caged Ca^{2+} compound NP-EGTA was washed out of the cytoplasm after introducing a drug-free solution into a rod through a patch pipette. The inset diagram illustrates the experimental configuration. The ER of an isolated rod was first loaded by incubation for 2.5 h with NP-EGTA AM (10 μM; purple). Rods were then patch clamped to wash NP-EGTA out of the cytoplasm and introduce fluo-5F (green) through the patch pipette to monitor cytoplasmic $[Ca^{2+}]$ changes. Flashing a spatially confined spot of UV light (6 μm in diameter, 1.5 ms) onto the soma three times in succession did not stimulate cytoplasmic Ca^{2+} increases. ***B***, When ryanodine (2 μM) was included in the pipette solution to stimulate the opening of RyR channels, uncaging Ca^{2+} from NP-EGTA in somatic ER with a small spot of UV light focused on the soma stimulated a rapid Ca^{2+} increase in somatic cytoplasm caused by diffusion of Ca^{2+} out of the ER through open RyR channels (filled black circles). This increase in cytoplasmic Ca^{2+} in the soma was followed by a slower increase in terminal cytoplasmic Ca^{2+} (open red circles). The increase in terminal cytoplasmic Ca^{2+} caused by uncaging Ca^{2+} in somatic ER was modeled as diffusion through a pipe using the equation in Results (blue line). The diffusion coefficient for the movement of Ca^{2+} ($D_{Ca^{2+}}^{Mix}$) through the axon from soma to terminal (12.4 μm) was 31 $\mu m^2/s$ in this example. The inset diagram illustrates a rod loaded with the caged Ca^{2+} compound NP-EGTA AM in the ER (purple). The cytoplasm was loaded with OGB-6F (green, 500 μM) and ryanodine (Ry) through a patch pipette. Unlike the other experiments in this figure, this experiment was conducted with rods in retinal slices. ***C***, Abruptly increasing Ca^{2+} in somatic ER (black) caused a secondary slow rise of Ca^{2+} in terminal ER (red). The increase in terminal ER Ca^{2+} caused by localized photolytic Ca^{2+} uncaging in somatic ER was modeled with the equation in Results (blue), yielding a diffusion coefficient ($D_{Ca^{2+}}^{ER}$) for movement of Ca^{2+} through the ER from soma to terminal (6 μm) of 25 $\mu m^2/s$. The diagram shows a rod loaded with both fluo-5N AM (green) and NP-EGTA AM (purple) in the ER. fluo-5N and NP-EGTA were washed out of the cytoplasm of the isolated rod with a dye- and drug-free solution in the patch pipette. ***D***, Abruptly increasing Ca^{2+} in somatic cytoplasm (black trace) by flash photolysis of NP-EGTA with a small spot of UV light focused on the soma was followed by a slower secondary rise of Ca^{2+} in terminal cytoplasm (red trace). To examine diffusion of cytoplasmic $[Ca^{2+}]$, isolated rods were loaded for 1 h with fluo-4 AM (green cross-hatching) and NP-EGTA AM (purple cross-hatching). Fitting the increase in terminal cytoplasmic Ca^{2+} with the equation in Results (blue line) yielded a $D_{Ca^{2+}}^{Cyto}$ of 33 $\mu m^2/s$ in this cell in which the distance from the soma/axon border to the center of the terminal was 13.4 μm.

performed control experiments in which we monitored cytoplasmic $[Ca^{2+}]$ changes by including membrane-impermeant fluo-5F or OGB-6F salts in the pipette solution. After waiting at least 3 min after patch rupture, flashing a confined spot of UV light (6 μm diameter) onto the soma did not evoke $[Ca^{2+}]$ increases in either somatic or terminal cytoplasm of isolated rods ($n = 6$; Fig. 4*A*) or rods from retinal slices ($n = 6$). The transients in the example in Figure 4*A* were artifacts of the brief uncaging flashes.

We next loaded the ER of rods from retinal slices with NP-EGTA and monitored cytoplasmic Ca^{2+} with OGB-6F salts introduced through the patch pipette. This is similar to the experimental configuration described in Figure 4*A* except that we also included 2 μM ryanodine in the patch pipette solution to activate RyRs and thus permit Ca^{2+} to exit from the ER into the cytoplasm. When ryanodine was included in the pipette solution, localized uncaging of Ca^{2+} in the somatic ER by application of a spatially confined UV light flash stimulated an abrupt increase in cytoplasmic Ca^{2+} of the soma (Fig. 4*B*, filled black circles), followed by a secondary slow rise in terminal cytoplasmic Ca^{2+} (Fig. 4*B*, open red circles). As shown by the control experiments in Figure 4*A*, this increase in cytoplasmic Ca^{2+} was not attributable to residual NP-EGTA in the cytoplasm but was instead a consequence of uncaging Ca^{2+} within the ER, followed by diffusion of Ca^{2+} ions out of the ER and into the cytoplasm through open RyR channels. The slow increase in terminal cytoplasmic Ca^{2+} was attributable to diffusion of Ca^{2+} down the axon. This could be a result of diffusion through the cytoplasm or diffusion through the ER lumen, followed by exit into the cytoplasm through open RyR channels in the terminal.

We estimated the diffusion coefficient for Ca^{2+} movement down the axon by modeling this process as diffusion through a pipe using the following formula (Berg, 1983): $F(t) = F_{max}/2[1 - \mathrm{erf}(x/4Dt)^{1/2})]$, where $F(t)$ is the fluorescence at each point in time, F_{max} is the plateau fluorescence value, x is the distance from the soma/axon boundary to the center of the terminal, and t is time. The error function (erf) was approximated numerically (Abramowitz and Stegun, 1972, their Eq. 7.1.27), and data were fit by nonlinear regression. This analysis yielded a diffusion coefficient ($D^{Mix}_{Ca^{2+}}$) of 30.6 ± 4.1 $\mu m^2/s$ ($n = 5$; Fig. 4*B*, blue line; Table 1).

We next studied $[Ca^{2+}]$ changes within the ER by loading the ER of isolated rods with both fluo-5N AM and NP-EGTA AM for 2.5 h and then washing both compounds out of the cytoplasm by introducing a dye- and drug-free patch pipette solution. Photolytic uncaging of NP-EGTA in the soma with a spatially confined UV light flash stimulated an abrupt, large Ca^{2+} increase in somatic ER (Fig. 4*C*, black). This direct elevation of Ca^{2+} in somatic ER caused by localized photolytic activation of NP-EGTA in somatic ER was followed by a slower secondary increase in terminal ER Ca^{2+} (Fig. 4*C*, red). The slow rise in terminal ER Ca^{2+} that followed Ca^{2+} uncaging in somatic ER was fit with equation above, yielding $D^{ER}_{Ca^{2+}}$ of 23.1 ± 2.9 $\mu m^2/s$ ($n = 14$; Fig. 4*C*; Table 1). Uncaging flashes applied directly to the terminal evoked only small intraterminal Ca^{2+} increases that were not sufficient to stimulate a detectable secondary Ca^{2+} increase in the soma ($n = 3$ cells).

For comparison, we also measured diffusion of Ca^{2+} through the cytoplasm by loading isolated rods with both fluo-4 AM and NP-EGTA-AM for 1 h (Fig. 4*D*). The shorter incubation time was used to minimize loading into the ER, and the higher Ca^{2+} affinity fluo-4 was chosen to limit measurements to cytoplasmic Ca^{2+} changes because high levels of Ca^{2+} in the ER (Bygrave and Benedetti, 1996) would be expected to saturate fluo-4. Uncaging Ca^{2+} from cytoplasmic NP-EGTA in the soma stimulated an abrupt increase in cytoplasmic $[Ca^{2+}]$ in the soma (Fig. 4*D*, black). This abrupt rise in somatic $[Ca^{2+}]$ was followed by a delayed increase in terminal cytoplasmic $[Ca^{2+}]$ (Fig. 4*D*, red). The slower increase in terminal cytoplasmic $[Ca^{2+}]$ caused by uncaging Ca^{2+} in soma cytoplasm was presumably attributable to diffusion of Ca^{2+} through axonal cytoplasm. Fitting the intraterminal increase in cytoplasmic $[Ca^{2+}]$ with equation above (Fig. 4*D*, blue line) yielded a diffusion coefficient ($D^{Cyto}_{Ca^{2+}}$) of 32.6 ± 7.3 $\mu m^2/s$ ($n = 8$; Table 1) for Ca^{2+} movement from soma to terminal through the cytoplasm.

The diffusion coefficient values found in the three uncaging experiments were similar to one another ($p = 0.26$, ANOVA; Table 1), and so differences in diffusion coefficient could not be used to distinguish whether the secondary increase in terminal cytoplasmic Ca^{2+} in the presence of open RyRs (Fig. 4*B*) was attributable to diffusion of Ca^{2+} through axonal cytoplasm, axonal ER, or both. The finding that $D^{Cyto}_{Ca^{2+}}$ and $D^{ER}_{Ca^{2+}}$ were similar to one another ($p = 0.17$, *t* test) suggests that Ca^{2+} ions can move with relative freedom through the ER from soma to terminal.

Discussion

ER forms a single continuous Ca^{2+} store throughout rods

FRAP and FLIP experiments with fluo-5N confirmed that the ER forms a continuous structure in rods that allows for the diffusion of small molecules from soma to terminal (Mercurio and Holtzman, 1982; Ungar et al., 1984; Chen et al., 2014). The time constant for recovery of fluo-5N fluorescence within the ER after localized photobleach was threefold slower than recovery of cytoplasmic fluo-4 fluorescence, presumably because of the greater tortuosity of the ER lumen compared with the cytoplasm. Similarly, diffusion of fluo-5N through the sarcoplasmic reticulum (SR) of cardiac myocytes is 3- to fourfold slower than cytoplasmic diffusion (Wu and Bers, 2006). Although dye diffusion coefficients differed between ER and cytoplasm, the Ca^{2+} diffusion coefficients $D^{ER}_{Ca^{2+}}$ (23 $\mu m^2/s$) and $D^{Cyto}_{Ca^{2+}}$ (33 $\mu m^2/s$) were not significantly different. $D^{Cyto}_{Ca^{2+}}$ was similar to a previous estimate derived from the spread of Ca^{2+} waves through rod terminals (34–40 $\mu m^2/s$; Cadetti et al., 2006). In cardiac myocytes, Swietach et al. (2008) calculated $D_{Ca^{2+}}$ in SR of 8–9 $\mu m^2/s$, slightly less than the cytoplasmic $D_{Ca^{2+}}$ of 14 $\mu m^2/s$ (Wu and Bers, 2006). However, other studies in cardiac myocytes have found a much higher value for $D_{Ca^{2+}}$ in the SR (60 $\mu m^2/s$; Wu and Bers, 2006; Picht et al., 2011). Studies on pancreatic acinar cells also found that Ca^{2+} diffuses through the ER more freely than through the cytoplasm (Park et al., 2000). This is thought to be attributable to weaker Ca^{2+} binding in the ER (Mogami et al., 1999; Wu and Bers, 2006; Picht et al., 2011). The finding that $D^{ER}_{Ca^{2+}}$ and $D^{Cyto}_{Ca^{2+}}$ of rods are similar to one another suggests that the low affinity of Ca^{2+} binding sites within the ER may compensate for effects of spatial tortuosity and allow relatively free movement of Ca^{2+} through the ER.

Ca^{2+} in somatic ER helps replenish depleted Ca^{2+} stores in terminals

We found that localized depletion of intraterminal ER Ca^{2+} (stimulated by local ryanodine puffs or modest membrane depolarization) was followed by a secondary reduction in somatic ER Ca^{2+}. The decrease in ER Ca^{2+} in the soma appeared larger than the corresponding increase in cytoplasmic Ca^{2+} in the soma. This could reflect dilution of Ca^{2+} into the cytoplasmic volume but could also be explained by diffusion of Ca^{2+} through the ER from soma to terminal. With maintained depolarization, there was a greater Ca^{2+} decline in terminal ER than somatic ER, indicating that a gradient of Ca^{2+} developed between the soma and terminal ER. This concentration gradient would drive Ca^{2+} through the ER from soma to terminal. Because Ca^{2+} ions diffuse through the ER from the soma to replenish ions depleted from terminal ER during CICR, Ca^{2+} may be simultaneously restored to the ER in the soma and other parts of the cell by store-operated Ca^{2+} entry (SOCE) across the plasma membrane (Szikra et al., 2008; García-Sancho, 2014) and uptake of Ca^{2+} into the ER via SERCA2 (Krizaj, 2005; Szikra and Krizaj, 2007). Although we did not investigate this possibility directly, the small slow Ca^{2+} increase in soma cytoplasm observed after activation of CICR and depletion of Ca^{2+} stores in the terminal may involve SOCE. Contributions of SOCE to maintaining ER Ca^{2+} levels and the diffusion of Ca^{2+} from soma to terminal may explain why blocking SOCE channels, like blocking CICR, inhibited slower components of glutamate release from rods but had little effect on fast, transient release evoked by brief depolarizing steps (Szikra et al., 2008).

In rods, Ca^{2+} released from terminal ER stores can trigger vesicle fusion at both ribbon and non-ribbon sites (Suryanarayanan and Slaughter, 2006; Chen et al., 2014), and at least 50% of the sustained glutamate release from both mammalian and amphibian rods in darkness appears to be driven by CICR (Cadetti et al., 2006; Suryanarayanan and Slaughter, 2006; Babai et al., 2010). Release from cones occurs only at ribbon sites and does not in-

volve CICR (Cadetti et al., 2006; Snellman et al., 2011). The continued influx of Ca^{2+} through L-type Ca^{2+} channels located deep within invaginating rod synapses causes a decline in synaptic cleft Ca^{2+} levels during sustained depolarization that is sufficient to cause a large reduction in I_{Ca} amplitude (Rabl and Thoreson, 2002). The remaining small influx of Ca^{2+} during sustained depolarization can be amplified by CICR (Krizaj et al., 1999, 2003), which in turn amplifies release (Cadetti et al., 2006; Suryanarayanan and Slaughter, 2006; Babai et al., 2010). The soma-to-terminal Ca^{2+} gradient that develops during sustained depolarization and the ability of Ca^{2+} to diffuse freely through the ER promotes the continuous refilling of intraterminal Ca^{2+} stores required to sustain CICR in rod terminals indefinitely during long periods of darkness. This mechanism of Ca^{2+} tunneling from soma to terminal through the ER appears to be essential for maintaining synaptic release from rods in darkness. Choi et al. (2006) showed that the ER extends from the soma into the dendrites of neurons. Our results showed that the ER network also extends from the soma into presynaptic terminals. This is consistent with findings from a number of other neurons showing submembrane cisterns of ER in both presynaptic and postsynaptic processes (Bouchard et al., 2003; Fuchs et al., 2014; Segal and Korkotian, 2014). CICR triggers release directly in rods (Suryanarayanan and Slaughter, 2006; Chen et al., 2014), in part because of the submicromolar affinity of the exocytotic Ca^{2+} sensor in photoreceptors (Thoreson et al., 2004). It is unclear whether CICR is capable of triggering release directly in other neurons, but it can provide a source of Ca^{2+} to enhance release (Verkhratsky, 2005; for review, see Castellano-Muñoz and Ricci, 2014). CICR in presynaptic terminals also contributes to synaptic plasticity and synaptic dysfunction in neurodegenerative diseases (for review, see Stutzmann and Mattson, 2011). In addition to providing a source of Ca^{2+}, the ER can also serve as a Ca^{2+} sink under certain conditions, limiting the influence of Ca^{2+} entering through ion channels (Castonguay and Robitaille, 2001; Im et al., 2014).

Our study focused on the ability of ER Ca^{2+} movements to sustain synaptic release, but free movement of Ca^{2+} through the ER can also communicate synaptic Ca^{2+} changes back to the soma to influence a diverse array of processes, including mitochondrial function, gene expression, and protein folding (Verkhratsky, 2005; Araki and Nagata, 2011; Kaufman and Malhotra, 2014). Bidirectional communication of Ca^{2+} within the ER between soma and terminal can impart beneficial adaptability to neurons but also contribute to damaging apoptotic and ER stress responses (Verkhratsky, 2005).

References

Abramowitz M, Stegun IA (1972) Handbook of mathematical functions with formulas, graphs, and mathematical tables. New York: Dover Publications.

Araki K, Nagata K (2011) Protein folding and quality control in the ER. Cold Spring Harb Perspect Biol 3:a007526. CrossRef Medline

Babai N, Morgans CW, Thoreson WB (2010) Calcium-induced calcium release contributes to synaptic release from mouse rod photoreceptors. Neuroscience 165:1447–1456. CrossRef Medline

Berg HC (1983) Random walks in biology. Princeton: Princeton UP.

Bers DM, Shannon TR (2013) Calcium movements inside the sarcoplasmic reticulum of cardiac myocytes. J Mol Cell Cardiol 58:59–66. CrossRef Medline

Bouchard R, Pattarini R, Geiger JD (2003) Presence and functional significance of presynaptic ryanodine receptors. Prog Neurobiol 69:391–418. CrossRef Medline

Bygrave FL, Benedetti A (1996) What is the concentration of calcium ions in the endoplasmic reticulum? Cell Calcium 19:547–551. CrossRef Medline

Cadetti L, Tranchina D, Thoreson WB (2005) A comparison of release kinetics and glutamate receptor properties in shaping rod–cone differences in EPSC kinetics in the salamander retina. J Physiol 569:773–788. CrossRef Medline

Cadetti L, Bryson EJ, Ciccone CA, Rabl K, Thoreson WB (2006) Calcium-induced calcium release in rod photoreceptor terminals boosts synaptic transmission during maintained depolarization. Eur J Neurosci 23:2983–2990. CrossRef Medline

Castellano-Muñoz M, Ricci AJ (2014) Role of intracellular calcium stores in hair-cell ribbon synapse. Front Cell Neurosci 8:162. CrossRef Medline

Castonguay A, Robitaille R (2001) Differential regulation of transmitter release by presynaptic and glial Ca^{2+} internal stores at the neuromuscular synapse. J Neurosci 21:1911–1922. Medline

Chen M, Van Hook MJ, Zenisek D, Thoreson WB (2013) Properties of ribbon and non-ribbon release from rod photoreceptors revealed by visualizing individual synaptic vesicles. J Neurosci 33:2071–2086. CrossRef Medline

Chen M, Križaj D, Thoreson WB (2014) Intracellular calcium stores drive slow non-ribbon vesicle release from rod photoreceptors. Front Cell Neurosci 8:20. CrossRef Medline

Choi YM, Kim SH, Chung S, Uhm DY, Park MK (2006) Regional interaction of endoplasmic reticulum Ca^{2+} signals between soma and dendrites through rapid luminal Ca^{2+} diffusion. J Neurosci 26:12127–12136. CrossRef Medline

Dayel MJ, Hom EF, Verkman AS (1999) Diffusion of green fluorescent protein in the aqueous-phase lumen of endoplasmic reticulum. Biophys J 76:2843–2851. CrossRef Medline

De Robertis E (1956) Electron microscope observations on the submicroscopic organization of the retinal rods. J Biophys Biochem Cytol 2:319–330. CrossRef Medline

De Robertis E, Franchi CM (1956) Electron microscope observations on synaptic vesicles in synapses of the retinal rods and cones. J Biophys Biochem Cytol 2:307–318. CrossRef Medline

Estrada de Martin P, Novick P, Ferro-Novick S (2005) The organization, structure, and inheritance of the ER in higher and lower eukaryotes. Biochem Cell Biol 83:752–761. CrossRef Medline

Freihöfer D, Körtje KH, Rahmann H (1990) Ultrastructural localization of endogenous calcium in the teleost retina. Histochem J 22:63–72. CrossRef Medline

Fuchs PA, Lehar M, Hiel H (2014) Ultrastructure of cisternal synapses on outer hair cells of the mouse cochlea. J Comp Neurol 522:717–729. CrossRef Medline

García-Sancho J (2014) The coupling of plasma membrane calcium entry to calcium uptake by endoplasmic reticulum and mitochondria. J Physiol 592:261–268. CrossRef Medline

Im GJ, Moskowitz HS, Lehar M, Hiel H, Fuchs PA (2014) Synaptic calcium regulation in hair cells of the chicken basilar papilla. J Neurosci 34:16688–16697. CrossRef Medline

Johnson JE Jr, Perkins GA, Giddabasappa A, Chaney S, Xiao W, White AD, Brown JM, Waggoner J, Ellisman MH, Fox DA (2007) Spatiotemporal regulation of ATP and Ca^{2+} dynamics in vertebrate rod and cone ribbon synapses. Mol Vis 13:887–919. Medline

Kaufman RJ, Malhotra JD (2014) Calcium trafficking integrates endoplasmic reticulum function with mitochondrial bioenergetics. Biochim Biophys Acta 1843:2233–2239. CrossRef Medline

Krizaj D (2005) Serca isoform expression in the mammalian retina. Exp Eye Res 81:690–699. CrossRef Medline

Krizaj D, Bao JX, Schmitz Y, Witkovsky P, Copenhagen DR (1999) Caffeine-sensitive calcium stores regulate synaptic transmission from retinal rod photoreceptors. J Neurosci 19:7249–7261. Medline

Krizaj D, Lai FA, Copenhagen DR (2003) Ryanodine stores and calcium regulation in the inner segments of salamander rods and cones. J Physiol 547:761–774. CrossRef Medline

Krizaj D, Liu X, Copenhagen DR (2004) Expression of calcium transporters in the retina of the tiger salamander (*Ambystoma tigrinum*). J Comp Neurol 475:463–480. CrossRef Medline

Ladman AJ (1958) The fine structure of the rod-bipolar cell synapse in the retina of the albino rat. J Biophys Biochem Cytol 4:459–466. CrossRef Medline

Mercurio AM, Holtzman E (1982) Smooth endoplasmic reticulum and other agranular reticulum in frog retinal photoreceptors. J Neurocytol 11:263–293. CrossRef Medline

Michalak M, Robert Parker JM, Opas M (2002) Ca^{2+} signaling and calcium

binding chaperones of the endoplasmic reticulum. Cell Calcium 32:269–278. CrossRef Medline

Mogami H, Nakano K, Tepikin AV, Petersen OH (1997) Ca^{2+} flow via tunnels in polarized cells: recharging of apical Ca^{2+} stores by focal Ca^{2+} entry through basal membrane patch. Cell 88:49–55. CrossRef Medline

Mogami H, Gardner J, Gerasimenko OV, Camello P, Petersen OH, Tepikin AV (1999) Calcium binding capacity of the cytosol and endoplasmic reticulum of mouse pancreatic acinar cells. J Physiol 518:463–467. CrossRef Medline

Park MK, Petersen OH, Tepikin AV (2000) The endoplasmic reticulum as one continuous Ca^{2+} pool: visualization of rapid Ca^{2+} movements and equilibration. EMBO J 19:5729–5739. CrossRef Medline

Petersen OH, Verkhratsky A (2007) Endoplasmic reticulum calcium tunnels integrate signalling in polarised cells. Cell Calcium 42:373–378. CrossRef Medline

Picht E, Zima AV, Shannon TR, Duncan AM, Blatter LA, Bers DM (2011) Dynamic calcium movement inside cardiac sarcoplasmic reticulum during release. Circ Res 108:847–856. CrossRef Medline

Rabl K, Thoreson WB (2002) Calcium-dependent inactivation and depletion of synaptic cleft calcium ions combine to regulate rod calcium currents under physiological conditions. Eur J Neurosci 16:2070–2077. CrossRef Medline

Rabl K, Cadetti L, Thoreson WB (2005) Kinetics of exocytosis is faster in cones than in rods. J Neurosci 25:4633–4640. CrossRef Medline

Schnapf JL, Copenhagen DR (1982) Differences in the kinetics of rod and cone synaptic transmission. Nature 296:862–864. CrossRef Medline

Segal M, Korkotian E (2014) Endoplasmic reticulum calcium stores in dendritic spines. Front Neuroanat 8:64. CrossRef Medline

Shoshan-Barmatz V, Orr I, Martin C, Vardi N (2005) Novel ryanodine-binding properties in mammalian retina. Int J Biochem Cell Biol 37:1681–1695. CrossRef Medline

Shoshan-Barmatz V, Zakar M, Shmuelivich F, Nahon E, Vardi N (2007) Retina expresses a novel variant of the ryanodine receptor. Eur J Neurosci 26:3113–3125. CrossRef Medline

Snellman J, Mehta B, Babai N, Bartoletti TM, Akmentin W, Francis A, Matthews G, Thoreson W, Zenisek D (2011) Acute destruction of the synaptic ribbon reveals a role for the ribbon in vesicle priming. Nat Neurosci 14:1135–1141. CrossRef Medline

Solovyova N, Verkhratsky A (2002) Monitoring of free calcium in the neuronal endoplasmic reticulum: an overview of modern approaches. J Neurosci Methods 122:1–12. CrossRef Medline

Somlyo AP, Walz B (1985) Elemental distribution in Rana pipiens retinal rods: quantitative electron probe analysis. J Physiol 358:183–195. CrossRef Medline

Stutzmann GE, Mattson MP (2011) Endoplasmic reticulum Ca(2+) handling in excitable cells in health and disease. Pharmacol Rev 63:700–727. CrossRef Medline

Suryanarayanan A, Slaughter MM (2006) Synaptic transmission mediated by internal calcium stores in rod photoreceptors. J Neurosci 26:1759–1766. CrossRef Medline

Swietach P, Spitzer KW, Vaughan-Jones RD (2008) Ca^{2+}-mobility in the sarcoplasmic reticulum of ventricular myocytes is low. Biophys J 95:1412–1427. CrossRef Medline

Szikra T, Krizaj D (2007) Intracellular organelles and calcium homeostasis in rods and cones. Vis Neurosci 24:733–743. CrossRef Medline

Szikra T, Cusato K, Thoreson WB, Barabas P, Bartoletti TM, Krizaj D (2008) Depletion of calcium stores regulates calcium influx and signal transmission in rod photoreceptors. J Physiol 586:4859–4875. CrossRef Medline

Thoreson WB, Rabl K, Townes-Anderson E, Heidelberger R (2004) A highly Ca^{2+}-sensitive pool of vesicles contributes to linearity at the rod photoreceptor ribbon synapse. Neuron 42:595–605. CrossRef Medline

Ungar F, Piscopo I, Holtzman E (1981) Calcium accumulation in intracellular compartments of frog retinal rod photoreceptors. Brain Res 205:200–206. CrossRef Medline

Ungar F, Piscopo I, Letizia J, Holtzman E (1984) Uptake of calcium by the endoplasmic reticulum of the frog photoreceptor. J Cell Biol 98:1645–1655. CrossRef Medline

Van Hook MJ, Thoreson WB (2013) Simultaneous whole-cell recordings from photoreceptors and second-order neurons in an amphibian retinal slice preparation. J Vis Exp 76:e50007. CrossRef Medline

Verkhratsky A (2005) Physiology and pathophysiology of the calcium store in the endoplasmic reticulum of neurons. Physiol Rev 85:201–279. CrossRef Medline

Wu X, Bers DM (2006) Sarcoplasmic reticulum and nuclear envelope are one highly interconnected Ca^{2+} store throughout cardiac myocyte. Circ Res 99:283–291. CrossRef Medline